Comparison of Irreversible Deformation and Yielding in Microlayers of Polycarbonate with Poly(methylmethacrylate) and Poly(styrene-co-acrylonitrile)

JULIA KERNS,[1] ALEX HSIEH,[2] ANNE HILTNER,[1] ERIC BAER[1]

[1] Department of Macromolecular Science and Engineering, and Center for Applied Polymer Research, Case Western Reserve University, Cleveland, Ohio 44106-7202

[2] Army Research Laboratory, Aberdeen Proving Ground, Maryland 21005-5069

Received 9 November 1999; accepted 9 December 1999

ABSTRACT: Microlayers of polycarbonate (PC) with poly(methylmethacrylate) (PMMA) or poly(styrene-co-acrylonitrile) (SAN) were processed with varying layer thicknesses. Adhesion between PC and PMMA was found to be an order of magnitude higher than between PC and SAN, as determined with the T-peel method. To probe the effect of the adhesion difference on yielding and deformation of PC/PMMA and PC/SAN microlayers, the macroscopic stress–strain behavior was examined as a function of layer thickness and strain rate, and the results were interpreted in terms of the microdeformation behavior. During yielding, crazes in thick SAN layers opened up into cracks; however, PC layers drew easily because local delamination relieved constraint at the PC/SAN interface. Adhesion of PC/PMMA was too strong for delamination at the interface when PMMA crazes opened up into cracks at low strain rates. Instead, PMMA cracks tore into neighboring PC layers and initiated fracture. At higher strain rates, good adhesion produced yielding of thick PMMA layers, a phenomenon not observed with thick SAN layers. The change in microdeformation mechanism of PMMA with increasing strain rate produced a transition in the yield stress of PC/PMMA microlayers. Microlayers of both PC/SAN and PC/PMMA with thinner layers (individual layers 0.3–0.6 μm thick) exhibited improved ballistic performance compared to microlayers with thicker layers (individual layers 10–20 μm thick), which was due to cooperative yielding of both components. © 2000 John Wiley & Sons, Inc. J Appl Polym Sci 77: 1545–1557, 2000

Key words: irreversible deformation; yielding; microlayers; polycarbonate; poly(methylmethacrylate); poly(styrene-co-acrylonitrile)

INTRODUCTION

Good adhesion in polymer blends and composites is generally considered desirable, due to improvements in stiffness and modulus. However, if the adhesion is too strong, it can be detrimental to ductility. Many examples in the literature reveal the effect of adhesion on yielding of blends and composites. For example, in a study of polypropylene/glass fiber composites, Sova[1] found that a composite with lower interfacial adhesion had a lower yield stress and higher ductility than a composite with better adhesion. Lower interfacial adhesion allowed the polypropylene to yield without constraint of the glass fibers, which debonded

Correspondence to: A. Hiltner.

Contract grant sponsor: Army Research Office. Contract grant number: DAAG55-98-1-0311.

Contract grant sponsor: National Science Foundation. Contract grant number: DMR97-05696.

Journal of Applied Polymer Science, Vol. 77, 1545–1557 (2000)

from the matrix during deformation. With good adhesion between fiber and matrix, the glass fibers constrained yielding of the polypropylene, resulting in a higher yield stress. Fracture occurred shortly after the yield point. In another study of polypropylene/glass fiber composites, Kander and Siegmann[2] used strain rate to vary the adhesion between fiber and matrix. They found that at slow deformation rates, lower adhesion resulted in more ductile behavior. At higher strain rates, better adhesion enabled the glass fibers to constrain yielding of the polypropylene and relatively brittle behavior was observed.

The effect of adhesion on yielding was modeled by Li et al.[3] in studies of linear low density polyethylene blends with a dispersed, rigid polystyrene phase. Adhesion was varied by use of a compatibilizer. Uncompatibilized blends failed by interfacial debonding and void growth. In this case, a model based on a modified cross-sectional area successfully described the yield stress. The effect of constraint from the well-adhered PS particles in compatibilized blends was well described with a modified yield strain approach.[4]

If the yielding behavior of the components is similar and the adhesion is sufficient to allow stress transfer between phases, both phases in a polymer blend can yield. For example, blends of polycarbonate (PC) and poly(acrylonitrile-butadiene-styrene) (ABS) are compatible because of good interfacial adhesion of PC and poly(styrene-co-acrylonitrile) (SAN).[5,6] Santana et al.[7] found the interfacial adhesion was sufficient to cause both PC and ABS to yield. The yield stress followed the rule of mixtures.

Similarly, the yield stress of PC/poly(methylmethacrylate) (PMMA) blends obeyed the rule of mixtures because good adhesion ensured stress transfer between the components.[8] Good adhesion of PC and PMMA is exploited by use of a PMMA shell on core-shell impact modifiers for PC. Although both PMMA and SAN adhere well to PC, the effect of adhesion on yielding and deformation of PC/PMMA blends and PC/SAN blends has never been directly compared.

Microlayer coextrusion is an advanced processing technique that combines two or more polymers into alternating layers with layer thicknesses that can be controlled down to the submicron scale.[9–11] Microlayer coextrusion has advantages over conventional blending for studying the effects of adhesion. These advantages include large interfacial area with controlled geometry and size scale. Numerous studies of PC/SAN microlayers revealed the relation between macroscopic stress–strain properties and microdeformation mechanisms in this system.[12–17] A dramatic increase in toughness of PC/SAN was found as the number of layers increased. This was attributed to a change in the microdeformation mechanism to cooperative yielding of both PC and SAN as the individual layers became thinner.

The goal in this paper is to compare the effects of strain rate and layer thickness on the yielding and deformation of two microlayer systems with good adhesion: PC/PMMA and PC/SAN. Specifically, the role of adhesion on the macroscopic stress–strain curve and the microdeformation mechanisms of PC/SAN and PC/PMMA microlayers with thick layers (10–20 μm) was compared. The effect of strain rate on PC/PMMA microlayers with thick (10–20 μm) and thin (1–4 μm) layers was also examined. The possibility for improved toughness was explored by examining the effect of layer thickness on ballistic properties.

EXPERIMENTAL

PC was Calibre 300-15 (The Dow Chemical Company, Midland, MI) with a molecular weight of 27,000 g/mol, PMMA was V826-100 (Ato-Haas, Chicago, IL) with a molecular weight of 120,000 g/mol, and SAN was Tyril 867-B (The Dow Chemical Company, Midland, MI) with a molecular weight of 193,000 g/mol. The SAN composition, 25% acrylonitrile, was chosen for maximum adhesion to PC.[18]

The PC was dried in a vacuum oven at 100°C for 24 h prior to processing; PMMA and SAN were dried in a vacuum oven at 85°C for 24 h prior to processing. Microlayers of PC and PMMA with 32, 256, 1024, 2048, and 4096 layers, and microlayers of PC and SAN with 32 layers, were coextruded with the two-component microlayer system described previously.[9] The extruder temperatures were chosen so that the viscosities of PC and PMMA or SAN matched as they entered the feedblock. Both extruders were at 270°C for PC/PMMA microlayers, and the multiplier and exit die temperatures were slightly lower at 250°C. For PC/SAN microlayers, the extruder temperatures were 270°C for PC and 260°C for SAN, and the multipliers and exit die temperatures were held at 250°C. The composition of the microlayer was varied by changing the relative flow rates. The composition is given in parentheses as either the weight fractions or the nominal (calculated)

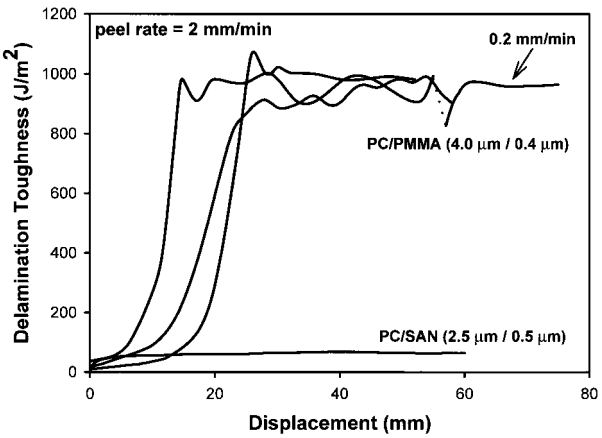

Figure 1 Peel curves of PC/SAN (2.5/0.5 μm) and PC/PMMA (4.0/0.4 μm).

layer thicknesses. For controls, PC and PMMA were extruded alone using the same processing conditions as the microlayers. The coextruded sheets were approximately 1 mm thick and 80 mm wide.

Previous peel studies of PC/SAN microlayers showed that adhesive failure occurred when the PC layer thickness was greater than 1.7 μm, and the SAN layer thickness was less than 1.5 μm.[19] Therefore, the PC/PMMA microlayer prepared for peel testing had 257 layers, a PC/SAN (90/10) composition and nominal layer thicknesses of 4.0 and 0.4 μm. The PC/SAN (85/15) with 1857 and nominal layer thicknesses of 2.5 and 0.5 μm used for peel testing was supplied by The Dow Chemical Company.

Tensile specimens were machined from the coextruded sheet parallel to the extrusion direction using a waisted geometry to localize deformation. The length of the waisted section was 60 mm and the width gradually decreased from 30 to 5 mm at the midpoint. Stress was calculated based on the minimum cross-sectional area at the center of the waisted specimen. Strain and strain rate were calculated using the length of the waisted section as the gage length. Tests were performed on an Instron testing machine at strain rates ranging from 0.1 to 100%/min. At least three specimens of each composition were tested.

Specimens for optical microscopy were prepared by cutting a 60 mm strip through the thickness of the microlayer parallel to the extrusion direction with a low-speed diamond saw. This resulted in a rectangular specimen 0.8–1.2 mm wide and 60 mm long. The cut specimens were polished on a metallurgical wheel using fine sandpaper and alumina oxide aqueous suspensions. The central part of the specimen was thinned to 0.4–0.6 mm to localize the deformation to this region. The polished specimen was clamped in a Polymer Laboratories Minimat microtensile tester for uniaxial tensile testing. The microtensile tester was mounted on the stage of an optical microscope so that the deformation process could be photographed. Strain and strain rate were calculated using the waisted length of the specimen, which ranged from 12 to 15 mm, as the gage length. Specimens were stretched at strain rates of 0.1%/min and 10%/min.

Delamination toughness was determined with the T-peel test (ASTM D1876). Specimens 8–15 mm wide were notched by pushing a fresh razor blade into the midplane of the sheet. Specimens were loaded at a rate of 2 mm/min. Some tests were interrupted and the crack tip region was sectioned perpendicular to the plane of the crack with a low-speed diamond saw. The sections were polished on a metallurgical wheel with wet sandpaper and alumina oxide aqueous suspensions and photographed in a transmission optical microscope. Matching peel surfaces were coated with 10 nm of gold for examination in a JEOL JSM 840A scanning electron microscope. To determine the surface composition, uncoated peel surfaces were examined with the Nicolet 800 FTIR spectrometer in the ATR mode with a germanium 60/60 crystal.

Ballistic impact measurements were carried out using a helium gas gun apparatus. A test specimen was mounted between two aluminum plates with a 2 in diameter opening, and the plates were firmly tightened. The sample holder was clamped in the center of the ballistic impact test apparatus, and the specimen was subjected to the impact of a fragment-simulating projectile

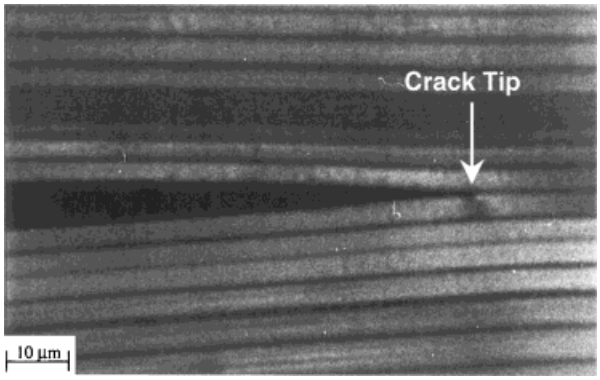

Figure 2 Crack tip of PC/PMMA (4.0/0.4 μm).

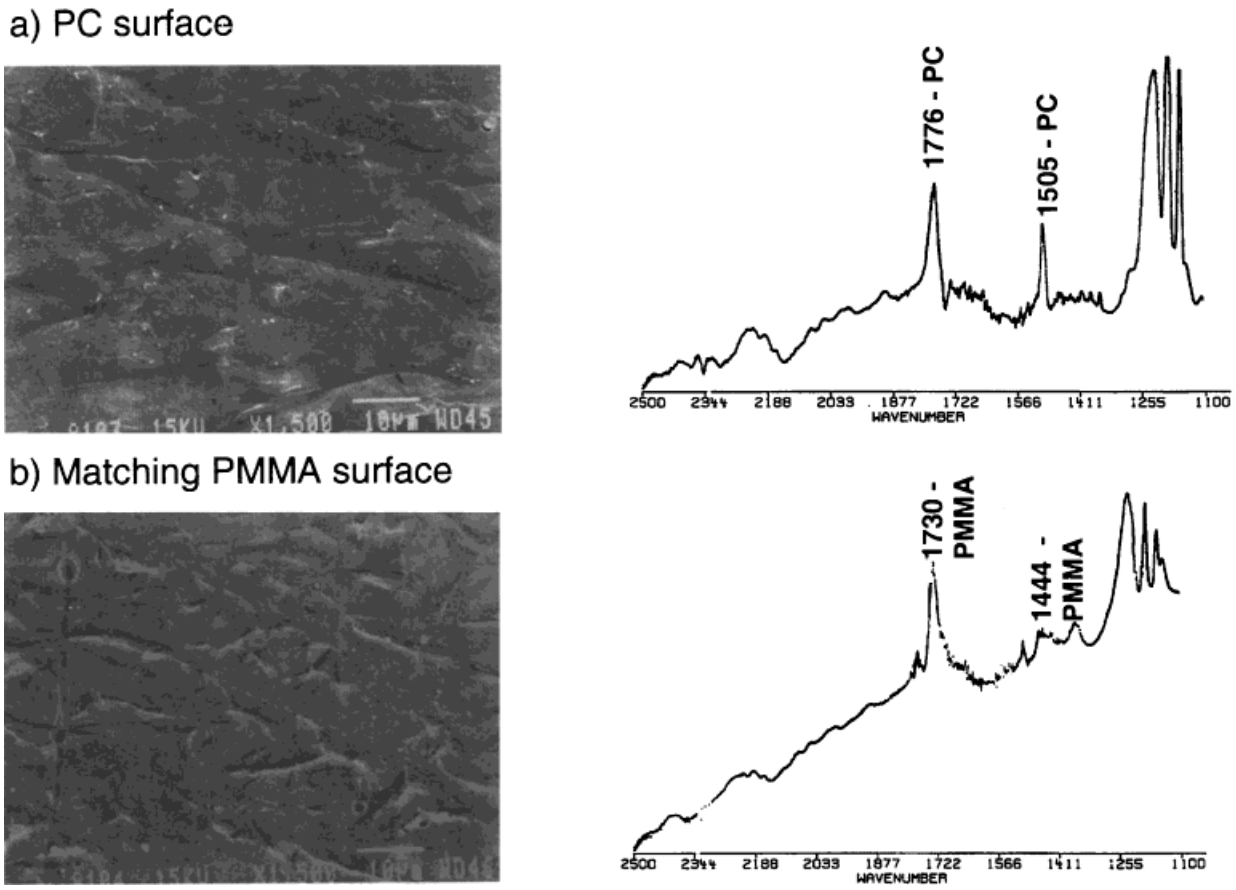

Figure 3 Matching peel surfaces and infrared spectra of PC/PMMA (4.0/0.4 μm) when the peel crack propagated: (a,b) along the PC-PMMA interface; (c,d) through a PMMA layer.

of 1.1 g weight and 0.22 in diameter. Four light screens were used as triggers for timers to record the time-of-flight of the projectile to determine the velocity of the projectile before and after impact. The impact velocities were between 120 and 160 m/s. Microlayers of PC/SAN (70/30) with 233, 929, and 1857 layers and approximately the same sheet thickness as the PC/PMMA microlayers were provided by The Dow Chemical Company.

RESULTS AND DISCUSSION

Delamination Toughness

Figure 1 compares peel curves for PC/PMMA (4.0/0.4 μm) and PC/SAN (2.5 /0.5 μm) tested at an extension rate of 2 mm/min. For both PC/PMMA and PC/SAN, test specimens were chosen with thick PC layers to insure that the peel crack did not propagate from layer to layer and thin SAN or PMMA layers to prevent crazing. A much higher force was required to propagate the crack in PC/PMMA than in PC/SAN. In PC/SAN, the curvature of the arms in the T-peel configuration conformed to the elastica shape,[20] and the arms fully recovered to their original shape after the test. The curvature of the PC/PMMA arms was much sharper than the elastica prediction, and the arms did not recover after the test was completed. The contribution of permanent deformation in the beam arms to the peel force was not accounted for in the peel curves shown.

Delamination toughness was calculated as $G = 2P_{cr}/W$ for a specimen of width W, where P_{cr} was the load at which the crack propagated. The PC/SAN microlayer failed with a delamination toughness of 70 J/m^2, which was comparable to the delamination toughness of 90 J/m^2 determined in past studies of PC/SAN microlayers with these layer thicknesses.[19] Inspection of the

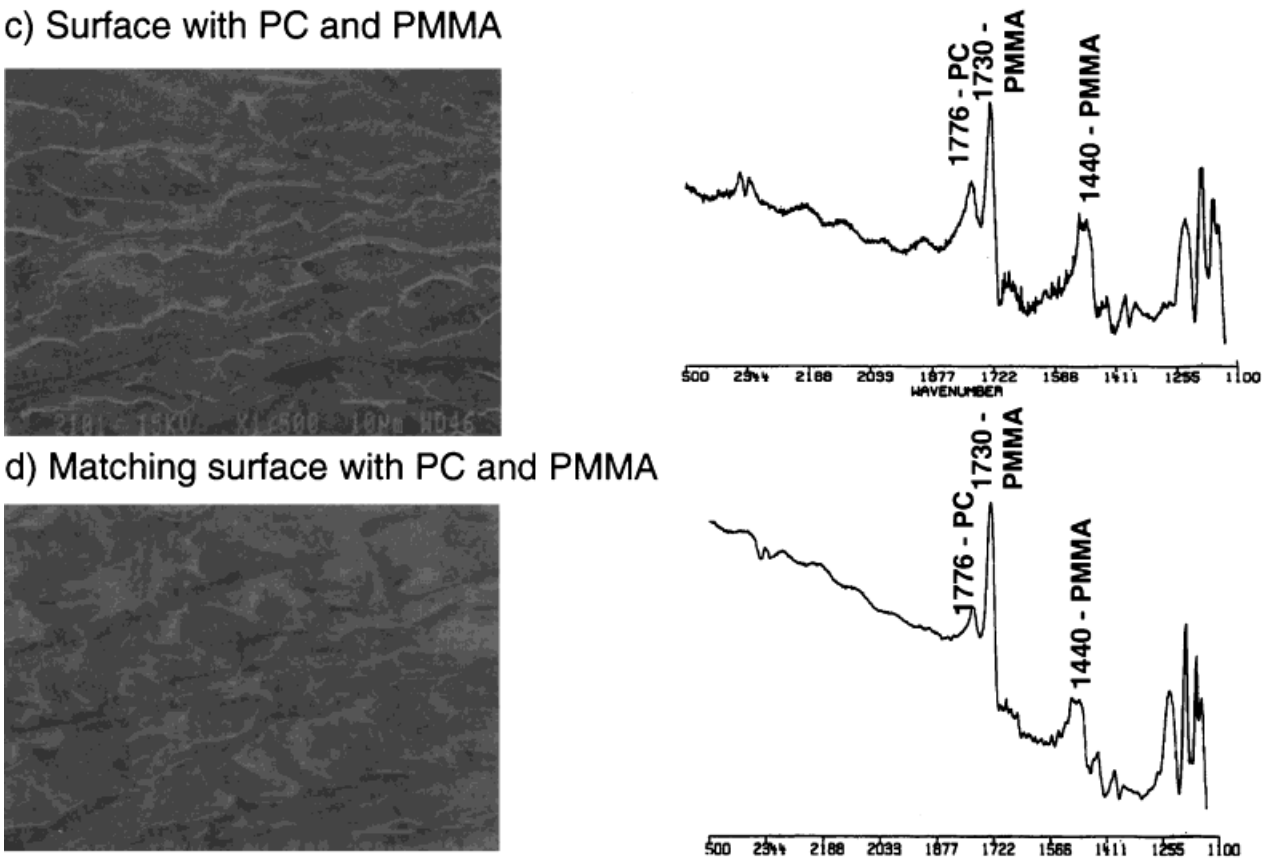

Figure 3 *(Continued from the previous page)*

fracture surfaces and peel crack tip showed that the crack propagated along one PC/SAN interface. Crazing in the SAN layers, which would have increased the measured delamination toughness, was not observed.

The PC/PMMA microlayer had a much higher delamination toughness of 950 J/m^2. The crack tip of the peel specimen (Fig. 2), showed no evidence of a craze damage zone at the crack tip. The crack ran along one PMMA layer and did not propagate through the PC layers.

The composition of the PC/PMMA peel surfaces was identified with attenuated total reflectance–Fourier transform IR. The strong carbonyl stretching bands at 1775 cm^{-1} for PC and 1730 cm^{-1} for PMMA were sufficiently separated that they could be used for this purpose. A specimen with a delamination toughness of 960 J/m^2 produced one peel surface with strong PC peaks at 1775 and 1505 cm^{-1}, indicating a PC-rich surface, and a corresponding peel surface with a strong peak at 1730 cm^{-1}, indicating a PMMA-rich surface, which confirmed interfacial failure [Fig. 3(a,b)]. Another specimen from the same microlayer with a delamination toughness of 870 J/m^2 showed strong PMMA absorptions at 1730 and 1440 cm^{-1} and a weak PC absorption at 1775 cm^{-1} from both surfaces [Fig. 3(c,d)]. This suggested that in this specimen, the peel crack propagated primarily through a PMMA layer.

Scanning electron micrographs showed a smooth PC surface in Figure 3(a), and a matching PMMA surface with some roughness in Figure 3(b). Consistent with interfacial failure, there was no evidence of tearing through multiple layers and no indication of crazing on the peel surfaces. The predominantly PMMA surfaces in Figure 3(c,d) resembled the PMMA surface from Figure 3(b). The high delamination toughness and combination of interfacial and cohesive failure suggested that the adhesive strength of PC/PMMA approached the cohesive strength of PMMA.

Previous investigators attributed the high fracture toughness of PC/PMMA joints to partial miscibility of PC and PMMA.[21] The miscibility of PC and PMMA has been debated[22–27]; however, the compelling evidence is that PC and PMMA are not miscible. Nevertheless, although the PC–

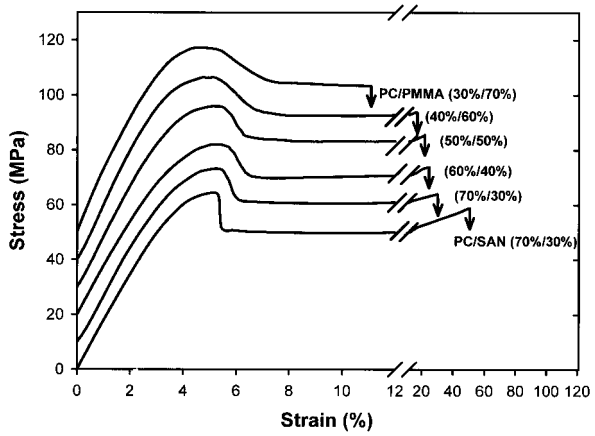

Figure 4 Stress–strain curves at 1%/min for 32-layer PC/PMMA specimens of various compositions, curves are shifted vertically by 10 MPa. A PC/SAN (70/30) specimen is included for comparison.

PMMA interaction is not as favorable as originally thought, their interaction is only weakly unfavorable for mixing.[27] This is consistent with observations of the PC/PMMA microlayer specimens, which have sharp layer boundaries but very good adhesion.

Stress–Strain Behavior of Microlayers with Thick Layers

The effect of PMMA content on the stress–strain curve of 32 layer PC/PMMA at a strain rate of 1%/min is shown in Figure 4. A 32 layer PC/SAN (70/30) microlayer is included for comparison. Differences were observed in yielding behavior as the composition was altered. For the PC/PMMA (70/30) specimen, yielding was indicated by a sharp stress drop on the stress–strain curve, although the drop was not as sharp as the stress drop for PC/SAN (70/30). As PMMA content increased, the yield maximum on the stress–strain curve broadened, so that specimens with the highest PMMA content had a much broader yield than those with lower PMMA content. This broadening of the yield with respect to composition was not observed with PC/SAN microlayers.[14] Differences in the stress–strain curve correlated with the appearance of the specimens. For PC/PMMA (70/30), formation of a neck was indicated by the appearance of a distinct macroscopic shear band, although it was not as sharp as the macroscopic shear band that accompanied neck formation of PC/SAN (70/30). As PMMA content increased, the process of thinning into a stable neck occurred more gradually. In fact, necking was so diffuse in specimens with the highest PMMA content that a well-defined neck was not obtained until the stress leveled off at the plateau on the stress–strain curve. For all compositions, the draw ratio was about 2.

All the specimens were ductile, and most of the PC/PMMA specimens fractured during neck propagation at about 20-30% strain, except for PC/PMMA (30/70), which fractured at about 11% strain. The PC/SAN (70/30) fractured at 50% strain, a higher strain than PC/PMMA with the same composition.

Figure 5 shows the stress–strain behavior of the PC/PMMA microlayers at a higher strain rate of 10%/min. Unlike the curves at 1%/min, the shape of the yield region was not affected by changing the PMMA composition. Instead, yielding was indicated by a sharp stress drop on the stress–strain curve and by formation of a neck from a macroscopic shearband regardless of composition. The PC/PMMA microlayers were ductile at this strain rate, although the fracture strain was lower than at 1%/min and decreased with increasing PMMA content from 20% for PC/PMMA (70/30) and (60/40) to 10% for microlayers with higher PMMA content.

The effect of strain rate on yield stress of PC/PMMA microlayers with 32 layers is shown in Figure 6. All PC/PMMA compositions tested at 1%/min, except PC/PMMA (30/70), yielded at about 63 MPa, which was close to the yield stress of PC, 60 MPa. The PC/SAN (70/30) tested at 1%/min yielded at 65 MPa, which was about the same yield stress as PC/PMMA. In contrast, the

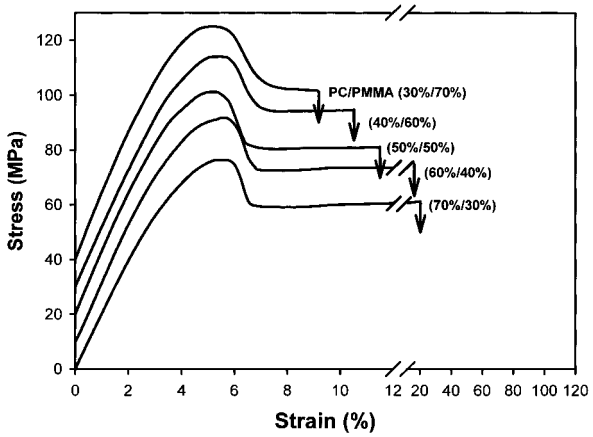

Figure 5 Stress–strain curves at 10%/min for 32-layer PC/PMMA specimens of various compositions, curves are shifted vertically by 10 MPa.

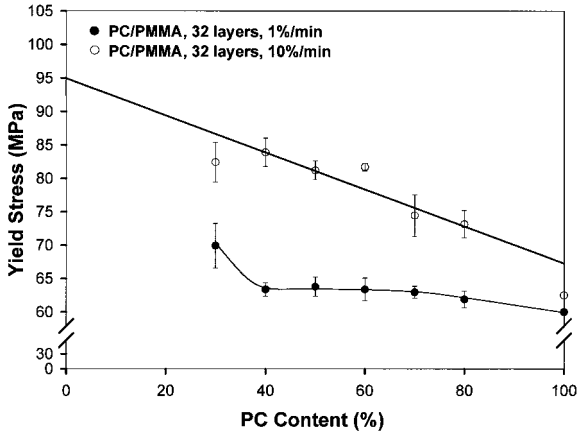

Figure 6 Effect of PC content on the yield stress of 32-layer PC/PMMA specimens at strain rates of 1 and 10%/min.

PC/PMMA microlayers tested at 10%/min exhibited an increase in yield stress with increasing PMMA content from 75 MPa for PC/PMMA (70/30) to 83 MPa for PC/PMMA (30/70). At this strain rate, the yield stress of the microlayers was intermediate between the yield stresses of PC and PMMA.[28] A linear relationship between yield stress and composition extrapolated to a PMMA yield stress of 95 MPa, which correlated with a value of 94 MPa obtained from high pressure tensile tests.[28]

Figure 7 compares the effect of strain rate on the yield stress of PC/SAN and PC/PMMA microlayers with the same 60/40 composition. At lower strain rates (0.1–1%/min) PC/PMMA and PC/SAN exhibited about the same yield stress with essentially no strain rate dependence. However, at higher strain rates (2–10%/min), the effect of strain rate on the yield stress was different for PC/PMMA and PC/SAN. The yield stress of PC/PMMA jumped from 63 MPa at 1%/min to 73 MPa at 2%/min and continued to increase with increasing strain rate. In contrast, the yield stress of PC/SAN gradually increased with increasing strain rate. It is reasonable to suggest that a change in yielding mechanism occurred in PC/PMMA, but not in PC/SAN, with increasing strain rate. All PC/PMMA compositions except PC/PMMA (30/70) showed this transition between strain rates of 1 and 2%/min.

Microdeformation of Thick Layers

The microdeformation behavior of individual PC and PMMA layers was observed in the optical microscope as the specimen was deformed. Specimens were tested at two rates, one on either side of the transition in yielding behavior. For specimens tested at 0.1%/min, the first visible irreversible deformation was crazing in the PMMA layers. As the strain increased, microshearbands initiated at the PC/PMMA interface where the craze tip in the PMMA layer impinged on the PC/PMMA interface and created a stress concentration. The shearbands grew partway across the PC layer. At the yield point, shearbands coalesced in the PC layers. Figure 8(a) shows the neck of a 32-layer PC/PMMA (70/30) specimen tested at 0.1%/min. Some of the PMMA crazes opened up into microcracks that tore into neighboring PC layers. No delamination failure occurred at the positions of high shear stress, indicated by arrows in Figure 8a. Some crazes remained closed. The uneven constraint imposed by the PMMA layers caused inhomogeneous extension of the PC layers and distortion of the PC/PMMA interface.

Figure 8(b) shows the necked specimen rotated 90° to expose a side view of the crazes in the PMMA layer. This view reveals that the microcracks were restricted to the surface. Instead of growing all the way through the specimen, they extended only to a depth of approximately 45 μm.

Specimens tested at 10%/min deformed much as specimens tested at 0.1%/min prior to yielding. Crazes formed in the PMMA layers; at the PC/PMMA interface shear bands initiated at the craze tips and grew across the PC layers. However, as shearbands coalesced in the PC layers, most of the PMMA crazes did not open up into microcracks, as shown in Figure 9(a). The PMMA

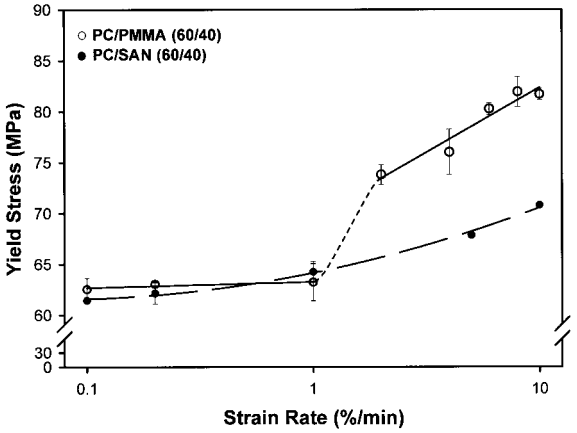

Figure 7 Effect of strain rate on the yield stress of PC/PMMA (60/40) and PC/SAN (60/40) 32-layer specimens.

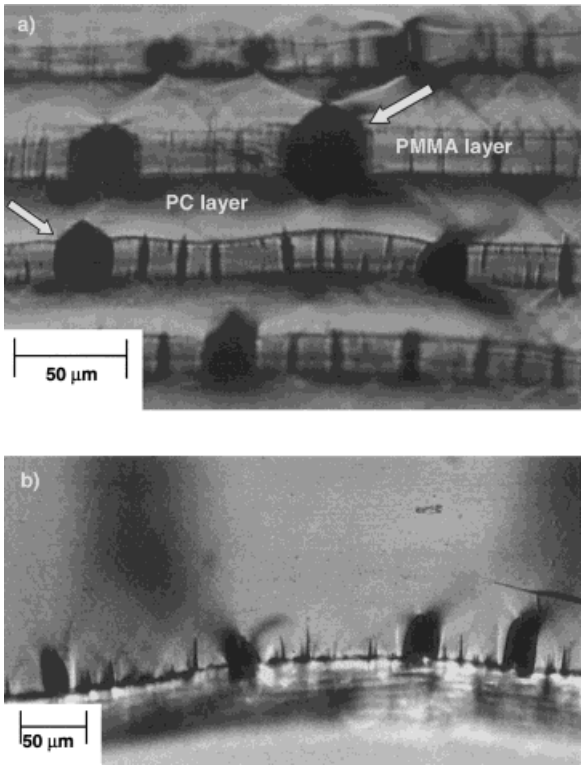

Figure 8 Optical micrographs of 32-layer PC/PMMA (70/30) tested at 0.1%/min showing (a) edge view of a necked specimen and (b) side view of a necked specimen. Arrows indicate positions of stress concentration.

layer thickness, which was measured before and after yielding, was reduced by 30%. This demonstrated that PMMA yielded. Arrows in Figure 9(a) highlight the absence of failure at the interface. The PC/PMMA interface was strong enough that crazes opened up in the center of the PMMA layer, but not at the interface.

Figure 9(b) shows a side view of the necked PC/PMMA specimen tested at 10%/min. No crazes were visible. Unlike specimens tested at 0.1%/min, the crazes did not extend to any significant depth below the surface. Only rarely did PMMA crazes open up into cracks. However, these isolated cracks initiated fracture.

This suggests an explanation for the difference in yield stress of specimens tested at lower and higher strain rates, a difference that was observed in the stress–strain curves of both macroscopic tensile bars and microdeformation specimens. At lower strain rates, a decrease in the effective cross-sectional area caused by PMMA surface cracks could account for the lower yield stress. Therefore an effective cross-sectional area was obtained by subtracting the depth of the cracks from the total thickness. The corrected yield stress σ_{yo} is given as

$$\sigma_{yo} = \sigma_y\left(\frac{A}{A_{eff}}\right) \quad (1)$$

where σ_y is the nominal yield stress at 0.1%/min, A is the original cross-sectional area, and A_{eff} is the area after the thickness of the cracks is subtracted. This correction reduced the original cross-sectional area by 14%. Using the effective cross-sectional area, the nominal yield stress of 63 MPa increased to 73 MPa, which was comparable to the yield stress of 75 MPa measured for a PC/PMMA (70/30) specimen tested at 10%/min.

The reason that PMMA crazes opened up into microcracks at low strain rates, but not at high strain rates, may relate to differences in craze microstructure at low and high strain rates. In a craze, the entangled polymer strands that bridge between neighboring fibrils can disentangle or break as the craze widens.[29] Alternatively, if there is a buildup of entangled strands, the strands may be pulled into cross-tie fibrils, i.e., short fibrils that bridge main fibrils.[30] The cross-tie fibrils increase the load-bearing capacity of the craze.

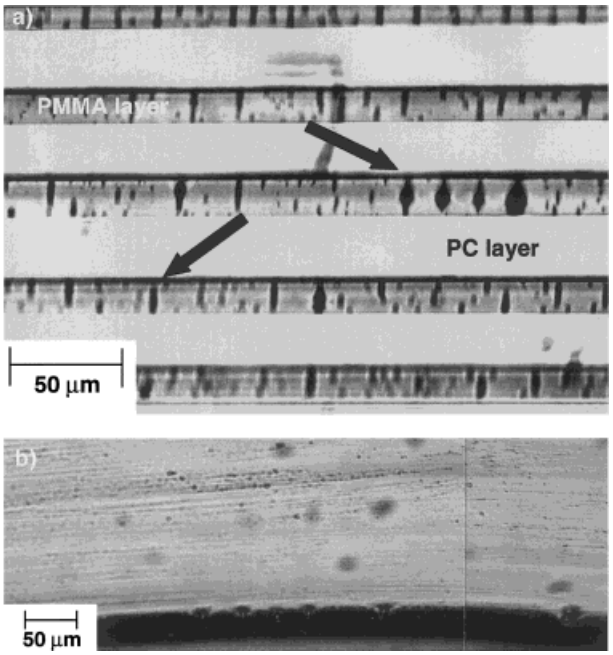

Figure 9 Optical micrographs of 32-layer PC/PMMA (70/30) tested at 10%/min showing (a) edge view of a necked specimen and (b) side view of a necked specimen. Arrows indicate positions of stress concentration.

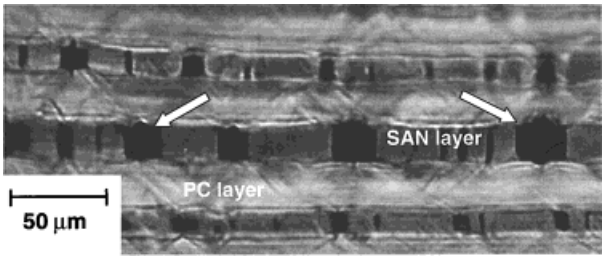

Figure 10 Optical micrograph of 32-layer PC/SAN (70/30) tested at 0.1%/min showing the edge view of the necked specimen. Arrows indicate local delamination.

A higher number of cross-tie fibrils may form at higher strain rates because entangled polymer strands have less time to disentangle. The cross-tie fibrils may strengthen the craze sufficiently that yielding is preferred over craze fracture. This is consistent with the finding of Miller et al.[31] that fewer cross-tie fibrils formed at higher temperatures, where chains disentangled more easily, than at lower temperatures.

A comparison of PC/PMMA with a PC/SAN microlayer of the same composition and layer thicknesses revealed the role of interfacial adhesion in the microdeformation behavior. Before the yield point, microdeformation of PC/SAN and PC/PMMA was essentially identical with crazing in the SAN layers followed by microshearband formation in the PC layers. As the shearbands coalesced and a stable neck formed at the yield point, SAN crazes opened up into microcracks. However, the SAN cracks did not cut into PC layers as the PMMA cracks did in PC/PMMA. Local delamination at the PC/SAN interface relieved the constraint of the SAN layers and permitted the PC layers to draw out. The interface was weak enough that the interfacial shear stress concentration caused local delamination as the specimen deformed, as indicated by the arrows in Figure 10. This contrasted with PC/PMMA shown in Figure 8(a), where the adhesion was strong enough to prevent even local delamination at the crack tip.

The difference in microdeformation behavior was manifest in the macroscopic stress–strain behavior. At lower strain rates, constraint imposed by PMMA on yielding of PC resulted in a diffuse neck. In contrast, local delamination of SAN relieved the constraint on yielding of PC and a sharp neck resulted. At low strain rates, the yield stress of PC/SAN and PC/PMMA microlayers was about the same because surface cracks in PC/SAN opened up to about the same depth as the surface cracks in PC/PMMA.[16] At higher strain rates, the yield stress of PC/PMMA increased abruptly when deformation of the PMMA layers changed from microcracking to yielding. The yield stress of PC/SAN microlayers did not similarly increase because the deformation mechanism of thick SAN layers did not change with strain rate.

Deformation of Microlayers with Thin Layers

The effect of layer thickness was revealed by comparing the stress–strain behavior of microlayers with 32 layers (individual layers 10–20 μm thick) and microlayers with 256 layers (individual layers 1–4 μm thick). The yield stress of PC/PMMA microlayers with 256 layers increased monotonically with increasing strain rate and increasing PMMA composition (Fig. 11). Comparing the yield stress of 256- and 32-layer specimens, the effect of strain rate on the yield stress was the same at higher strain rates but differed at lower strain rates. The 256-layer specimens did not show the transition between 1 and 2%/min strain rate that characterized the 32-layer specimens. The 256-layer specimens were also more ductile. Yielding occurred at the highest strain rate tested, 100%/min. However, the 32-layer specimens fractured before yielding at strain rates higher than 10%/min.

Examination of the microdeformation behavior of a 256-layer specimen at 0.1 %/min revealed craze arrays with aligned crazes in several neighboring PMMA layers, and cooperative shearbands that grew across several PC layers and the intervening PMMA layers. Figure 12 shows these fea-

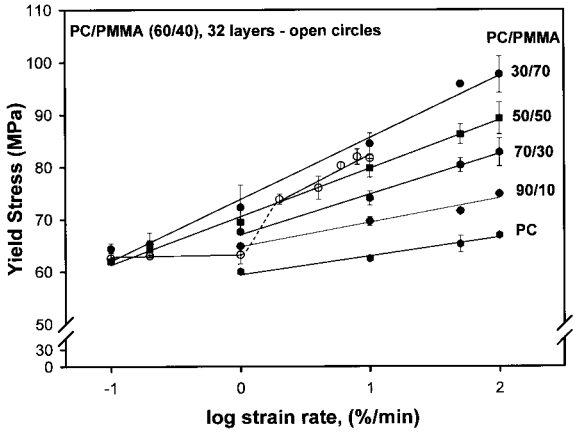

Figure 11 Effect of strain rate on the yield stress of 256-layer PC/PMMA of various compositions. The 32-layer PC/PMMA (60/40) is included for comparison.

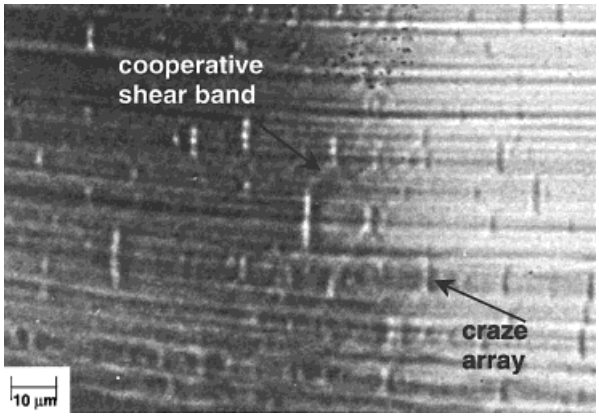

Figure 12 Optical micrographs of 256-layer PC/PMMA (70/30) tested at 0.1%/min showing the edge view.

tures in a PC/PMMA (70/30) specimen just before it necked. During yielding, the PMMA crazes remained closed as both PC and PMMA layers drew out. The same mechanism was seen in yielding of PC/SAN with thin layers. Yielding and drawing of both components was typical of PC/PMMA and PC/SAN microlayers with thin layers; however, the present study revealed that this mode of deformation could also occur in microlayers with thick layers, specifically in PC/PMMA microlayers tested at higher strain rates.

Comparison of the stress–strain curves of PC/PMMA (70/30) with 32, 256, and 2048 layers (individual layers 0.3–0.6 μm thick) at 50%/min revealed the effect of layer thickness on ductility (Fig. 13). The 32-layer specimens did not form a neck at this strain rate but rather fractured prior to yielding; however, 256- and 2048-layer specimens formed a stable neck and drew to higher strains before fracture. With increasing number of layers, fracture strain increased from 4% for 32 layers to 30% for 256 layers to 60% strain for 2048 layers. An increase in toughness with increasing number of layers was attributed in past studies of PC/SAN to cooperative shearbanding in the thinner layers.[12–16] It might be expected that PC/PMMA with 32 layers would be ductile at higher strain rates because cooperative shearbanding was observed. However, isolated surface crazes in the 32-layer specimens opened up into cracks and initiated fracture at low strains. This did not occur with thinner layers.

The effect of layer thickness on ductility was also examined in ballistic tests. Figure 14 shows specimens of PC/PMMA (80/20) and the PC control after ballistic impact. The PC control had good ballistic response. The projectile did not penetrate the specimen; dissipation of the impact energy away from the impact site left a circular impression where the specimen was clamped. The PC/PMMA (80/20) specimen with 256 layers fractured upon impact, an indication of poor ballistic response. Absence of a circular impression indicated that the material did not absorb much impact energy. Increasing the number of layers improved the ballistic performance. The projectile penetrated the 1024- and 2048-layer specimens, but the emergence of a circular impression showed that the material absorbed increasing amounts of impact energy. The 4096 layer specimen achieved the ballistic performance of the PC control. The projectile did not penetrate the specimen, and the circular impression where the specimen was clamped was evident. The absence of any delamination in the PC/PMMA specimens was attributed to the strong adhesion between PC and PMMA.

The ballistic performance of PC/SAN (70/30) also showed improvement with increasing number of layers (Fig. 15). Like PC/PMMA with 256 layers, PC/SAN with 233 layers fractured upon impact, an indication of poor ballistic response. Fracture of PC/SAN was accompanied by delamination, which was not observed with PC/PMMA, and was attributed to poorer adhesion between PC and SAN. The PC/SAN with 929 layers fractured with more profuse cracking and delamination, and emergence of a circular impression indicated that the specimen absorbed more impact energy. For PC/SAN with 1857 layers, the projectile did not penetrate the specimen and thus this microlayer achieved the ballistic performance of PC/PMMA with 4096 layers and the PC.

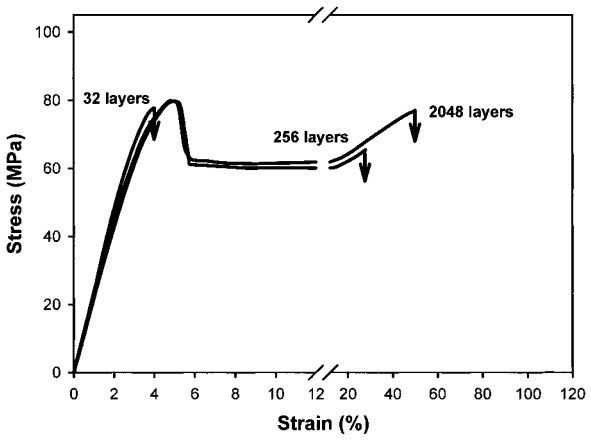

Figure 13 Stress–strain curves at 50%/min for PC/PMMA (70/30) with 32, 256, and 2048 layers.

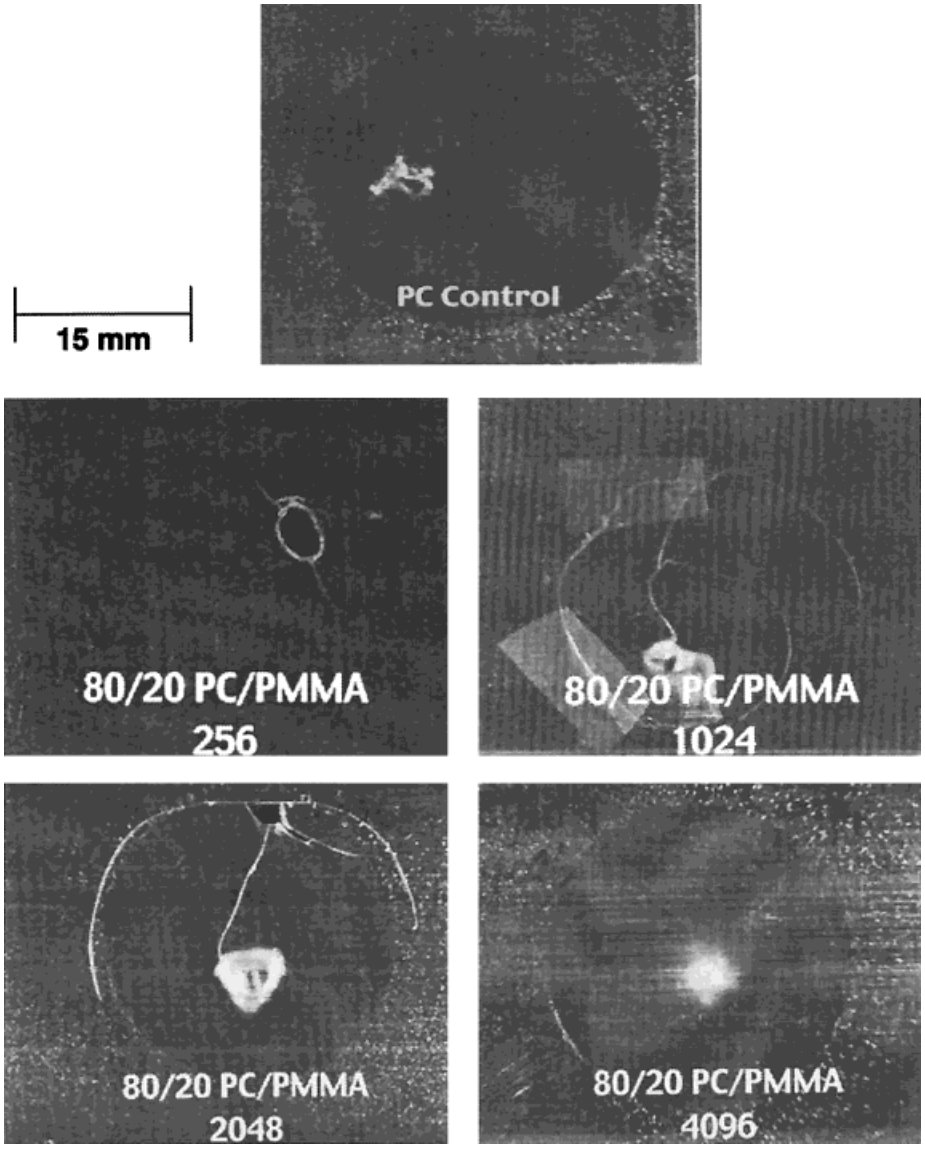

Figure 14 Ballistic specimens of PC/PMMA (80/20) with 256, 1024, 2048, and 4096 layers and the PC control.

CONCLUSIONS

Adhesion between PC and PMMA is considerably higher than between PC and SAN. For microlayers with thinner layers, the difference in adhesion had very little effect on the deformation mechanisms. Ductility of microlayers with thin layers was attributed to cooperative yielding of both components. This microdeformation mechanism was possible because adhesion between layers was sufficient to allow stress transfer across the PC/SAN or PC/PMMA interface. As a result, both PC/SAN and PC/PMMA microlayers with thin layers exhibited much better ballistic performance than microlayers with thicker layers.

However, the difference in adhesion of these two systems had direct consequences on deformation of microlayers with thicker layers. When crazes in SAN layers opened up into cracks during yielding, PC layers were able to draw easily because local delamination relieved constraint at the PC/SAN interface. Adhesion of PC/PMMA was too strong for delamination at the interface when PMMA crazes opened up into cracks at low strain rates. Instead, PMMA cracks tore into neighboring PC layers and initiated fracture. At

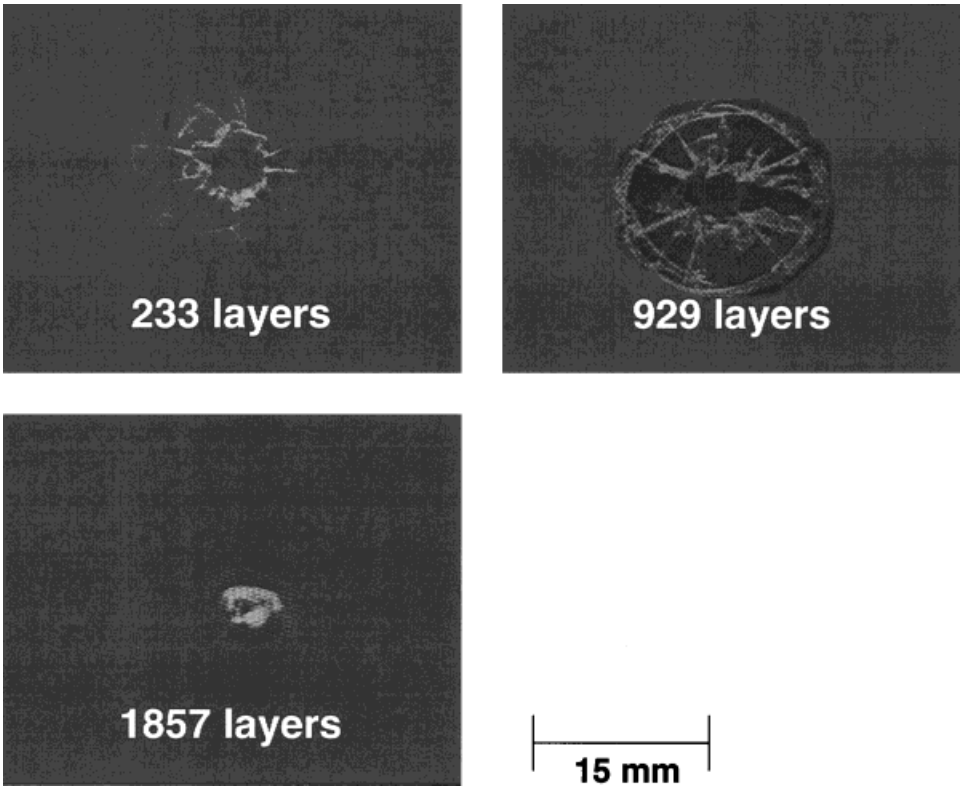

Figure 15 Ballistic specimens of PC/SAN (70/30) with 233, 929, and 1857 layers.

higher strain rates, PMMA crazes did not open up into cracks. Instead, good adhesion produced yielding of PMMA. The change in microdeformation mechanism of PMMA with changing strain rate produced a transition in PC/PMMA yield stress.

This work was generously supported by the Army Research Office (Grant DAAG55-98-1-0311) and the National Science Foundation (Grant DMR97-05696).

REFERENCES

1. Sova, M. J App Polym Sci 1989, 38, 511.
2. Kander, R. G.; Siegmann, A. J Compos Mat 1992, 26, 1455.
3. Li, T.; Topolkaraev, V. A.; Hiltner, A.; Baer E. In Toughened Plastics II; Riew, C. K.; Kinloch, A. J., Eds.; Advances in Chemisty Series 252; American Chemical Society: Washington, DC, 1996; p 319.
4. Li, T.; Carfagna, C.; Topolkaraev, V. A.; Hiltner, A.; Baer, E.; Ji, X. Z.; Quirk, R. P. In Toughened Plastics II; Riew, C. K., Kinloch, A. J., Eds.; Advances in Chemistry Series 252; American Chemical Society: Washington, DC, 1996; p 335.
5. Quintens, D.; Groeninckx, G.; Guest, M.; Aerts, L. Polym Eng Sci 1991, 31, 1215.
6. Koo, K. K.; Inoue, T.; Miyasaka, K. Polym Eng Sci 1985, 25, 741.
7. Santana, O. O.; Maspoch, M. M.; Martinez, A. B. Polym Bull 1998, 41, 721.
8. Kolarik, J.; Lednicky, F. Polym Eng Sci 1992, 32, 886.
9. Mueller, C.; Kerns, J.; Ebeling, T.; Nazarenko, S.; Hiltner, A.; Baer, E. In Polymer Process Engineering 97; Coates, P. D., Ed.; University Press: Cambridge, 1997; p 137.
10. Im, J.; Hiltner, A.; Baer, E. In High Performance Polymers; Baer, E., Moet, A., Eds.; Hanser: Munich, 1991; p 175.
11. Mueller, C.D.; Nazarenko, S.; Ebeling, T.; Hiltner, A.; Baer, E. Polym Eng Sci 1997, 37, 355.
12. Ma, M.; Vijayan, K.; Im, J.; Hiltner, A.; Baer, E. J Mater Sci 1990, 25, 2039.
13. Sung, K.; Haderski, D.; Hiltner, A.; Baer, E. J Appl Polym Sci 1994, 52, 147.
14. Gregory, B.L.; Siegmann, A.J.; Im, J.; Hiltner, A.; Baer, E. J Mater Sci 1987, 22, 532.
15. Haderski, D.; Sung, K.; Hiltner, A.; Baer E. J Appl Polym Sci 1994, 52, 121.
16. Sung, K.; Hiltner, A.; Baer, E. J Mater Sci 1994, 29, 5559.

17. Nazarenko, S.; Haderski, D.; Hiltner, A.; Baer, E. Macromol Chem Phys 1995, 196, 2563.
18. Keitz, J. D.; Barlow, J. W.; Paul, D. R. J Appl Polym Sci 1984, 29, 3131.
19. Hiltner, A.; Ebeling, T.; Shah, A.; Mueller, C.; Baer, E. In Interfacial Aspects of Multicomponent Polymer Materials; Lohse, D. J., Russell, T. P., Sperling, L. H., Eds.; Plenum: New York, 1997; p 95.
20. Kendall, K. J Adhes 1973, 5, 105.
21. Brown, H. R. J Mater Sci 1990, 25, 2791.
22. Kim, W. N.; Burns, C. N. Macromolecules 1987, 20, 1876.
23. Asano, A.; Takegoshi, K.; Hikichi, K. Polym J 1992, 24, 552.
24. Kolarik, J.; Lednicky, F. Polym Eng Sci 1992, 32, 886.
25. Kyu, T.; Saldanha, J. J Polym Sci: Part C: Polym Lett 1988, 26, 33.
26. Gardlund, Z. G. In Polymer Blends and Composites in Multiphase Systems; Han, C. D., Ed.; Advances in Chemisty Series 206; American Chemical Society: Washington, DC, 1984; p 129.
27. Nishimoto, M.; Keskula, H.; Paul, D. R. Polymer 1991, 32, 272.
28. Matsushige, K.; Radcliffe, S. V.; Baer, E. J Polym Sci 1976, 14, 703.
29. Kuo, C. C., Phoenix, S. L., Kramer, E. J. J Mater Sci Lett 1985, 4, 459.
30. Berger, L. L. Macromolecules 1989, 22, 3162.
31. Miller, P.; Buckley, D. J.; Kramer, E. J Mater Sci 1991, 26, 4445.